J Atmos Chem (2015) 72:261–286
DOI 10.1007/s10874-013-9257-6

Estimating surface NO_2 and SO_2 mixing ratios from fast-response total column observations and potential application to geostationary missions

T. Knepp · M. Pippin · J. Crawford · G. Chen · J. Szykman · R. Long · L. Cowen · A. Cede · N. Abuhassan · J. Herman · R. Delgado · J. Compton · T. Berkoff · J. Fishman · D. Martins · R. Stauffer · A. M. Thompson · A. Weinheimer · D. Knapp · D. Montzka · D. Lenschow · D. Neil

Received: 7 August 2012 / Accepted: 8 April 2013 /
Published online: 25 May 2013

Abstract Total-column nitrogen dioxide (NO_2) data collected by a ground-based sun-tracking spectrometer system (Pandora) and an photolytic-converter-based in-situ instrument

Jim Szykman is currently assigned to NASA Langley Research Center, Hampton, VA 23681, USA

T. Knepp (✉)
Science Systems and Applications, Inc., Hampton, VA 23681, USA
e-mail: travis.n.knepp@nasa.gov

T. Knepp · M. Pippin · J. Crawford · G. Chen · L. Cowen · D. Neil
NASA Langley Research Center, Hampton, VA 23681, USA

J. Szykman · R. Long
US EPA, Research Triangle Park, Durham, NC 27701, USA

A. Cede
LuftBlick, Kreith 6162, Austria

A. Cede · N. Abuhassan
NASA Goddard Space Flight Center, Greenbelt, MD 20771, USA

N. Abuhassan
School of Engineering, Morgan State University, Baltimore, MD 21251, USA

J. Herman · R. Delgado · J. Compton · T. Berkoff
Joint Center for Earth Systems Technology, University of Baltimore County, Baltimore, MD 21250, USA

J. Fishman
Department of Earth and Atmospheric Sciences, Saint Louis University, St. Louis, MO 63103, USA

D. Martins · R. Stauffer · A. M. Thompson
Department of Meteorology, Pennsylvania State University, University Park, PA 16802, USA

A. Weinheimer · D. Knapp · D. Montzka · D. Lenschow
National Center for Atmospheric Research, Boulder, CO 80305, USA

collocated at NASA's Langley Research Center in Hampton, Virginia were analyzed to study the relationship between total-column and surface NO_2 measurements. The measurements span more than a year and cover all seasons. Surface mixing ratios are estimated via application of a planetary boundary-layer (PBL) height correction factor. This PBL correction factor effectively corrects for boundary-layer variability throughout the day, and accounts for up to ≈75 % of the variability between the NO_2 data sets. Previous studies have made monthly and seasonal comparisons of column/surface data, which has shown generally good agreement over these long average times. In the current analysis comparisons of column densities averaged over 90 s and 1 h are made. Applicability of this technique to sulfur dioxide (SO_2) is briefly explored. The SO_2 correlation is improved by excluding conditions where surface levels are considered background. The analysis is extended to data from the July 2011 DISCOVER-AQ mission over the greater Baltimore, MD area to examine the method's performance in more-polluted urban conditions where NO_2 concentrations are typically much higher.

Keywords Nitrogen dioxide · Sulfur dioxide · Air quality · Remote sensing · DISCOVER-AQ · CAPABLE · GEO-CAPE

1 Introduction

Oxides of nitrogen and sulfur are key species in tropospheric chemistry. Nitrogen dioxide (NO_2), in particular, is a critical component in the process that leads to the formation of photochemical smog and tropospheric ozone (O_3), and thus greatly influences the troposphere's oxidizing capacity. Furthermore, NO_2 is the gas-phase precursor of nitric acid, which can lead to the formation of particles, influences greenhouse-gas mixing ratios, and has both direct and secondary impacts (via O_3 and particulate formation) on health and the environment (Krishna et al. 1997; Lin et al. 1988; Liu et al. 1987; Maheswaran et al. 2010; Meng et al. 1997; Thompson 1992). Rapidly changing, high-NO_2 events, on the order of hours, have been linked with significantly higher mortality in subsequent days, in addition to threats by chronic high-exposure (Amiot et al. 2012; Andersen et al. 2012; Brunekreef and Holgate 2002; Liu et al. 2012; van den Hooven et al. 2012). The health impacts from short-term exposure led the U.S. Environmental Protection Agency (EPA) to issue a new 1-hour National Ambient Air Quality Standard of 100 parts per billion (ppb, by volume) for NO_2 in 2010. Clearly, widespread monitoring of NO_2 due to its health impacts is highly important. However, establishing a surface NO_2 observation network capable of recording short time scale variability (i.e. on the order of minutes to an hour) with continental coverage is impractical. A practical alternative is making pollution observations from a geostationary satellite as currently planned in NASA's upcoming Geostationary Coastal and Pollution Events (GEO-CAPE) mission (Fishman et al. 2012). Indeed, satellite-based tropospheric-NO_2 measurements from GOME, SCIAMACHY (Ghude et al. 2009), GOME-2, and OMI (Fishman et al. 2008; Richter et al. 2005) have captured the global distribution of NO_2 and illustrate the importance of anthropogenic emissions on tropospheric O_3, particulate matter, and the environment. Recent global model analyses have demonstrated good agreement between OMI-derived tropospheric NO_2 columns and ground-level measurements on a monthly–seasonal basis (Lamsal et al. 2008, 2010; Ordonez et al. 2006; Petritoli et al. 2004), and Boersma et al. (2009) used surface NO_2 data to derive a boundary-layer column to show how OMI and SCIAMACHY capture intra-day variability caused by NO_2's diurnal variation. However, current satellite pixel footprints are large (13×24 km and 40×80 km for OMI (nadir view) and GOME-2 respectively), which can significantly bias the

representation of ground conditions (Irie et al. 2012; Noguchi et al. 2009). Satellite measurements, such as GEO-CAPE, with better temporal coverage (on the order of hours) and spatial resolution are still needed to resolve diurnal and horizontally heterogeneous features associated with the sources and transport of NO_2. From a health perspective, column-density observations are less informative than surface mixing ratios. Therefore, the question remains whether high temporal-resolution observations/estimates of surface-pollutant mixing ratios can be made from space.

A primary challenge in the use of satellite-based column data for air-quality and emissions monitoring applications is relating total-column observations to ambient surface mixing ratios. Elucidation of the column density to surface mole–fraction relationship, from a remote-sensing perspective, will allow comparison with surface mixing ratio measurements, which are often compared against a numerical metric associated with an established ambient air-quality standard. A significant challenge is accounting for variability in the planetary boundary layer (PBL) height, and relating variability in the column to changes in surface mixing ratios. In the early-morning hours, the PBL is shallow due to lack of turbulent mixing from surface heating. As a result, surface emissions during this time are confined to a relatively low layer near the ground, which allows the mixing ratios of emitted pollutants to increase more than they would if emitted later in the day as the PBL height increases due to daytime surface heating. Indeed, it is this PBL-height variability that introduces a disconnect between total-column observations and surface mixing ratio, which is important from a health (Amiot et al. 2012; Andersen et al. 2012; Brunekreef and Holgate 2002; Liu et al. 2012; van den Hooven et al. 2012), and attainment perspective as opposed to emission-trend studies (e.g. Richter et al. 2005; Zhang et al. 2007; Schneider and van der A 2012).

Past studies (e.g. Luo et al. 2012; Piters et al. 2012; Halla et al. 2011; Lee et al. 2011; Lamsal et al. 2008; Kramer et al. 2008; Leigh et al. 2007; Koelemeijer et al. 2006; Ordonez et al. 2006; Petritoli et al. 2004) that have compared column observations (i.e. satellite and surface-based MAX-DOAS instruments for chemical and aerosol species) with surface observations have utilized complex chemical transport models and/or large averaging times (weekly, seasonal, or annual) that effectively average out the influence of PBL variability and remove applicability of these observations to short-term, health related, NO_2 fluctuations that occur on the order of minutes to hours. In this study we compare column-density measurements derived from a ground-based spectrometer system (Herman et al. 2009) that has ~90 s resolution, with coincident surface mixing ratio measurements recorded every minute. We then present a methodology developed for the analysis of data collected at NASA's Langley Research Center (LaRC) between July 2010 and October 2011, and the July 2011 Deriving Information on Surface Conditions from COlumn and VERtically Resolved Observations Relevant to Air Quality (DISCOVER-AQ) field campaign in Baltimore, MD to convert a total-column observation to a surface mixing ratio estimate, and determine whether short-term surface NO_2 variability can be qualitatively and quantitatively observed in column observations that have short integration times.

2 Locations

The data for this study were collected at three locations: Hampton, VA, Padonia, MD, and Edgewood, MD. The Hampton measurements were obtained from July 2010

through October 2011, whereas the two Maryland datasets were obtained during the July 2011 DISCOVER-AQ field campaign.

2.1 Hampton, VA

Ongoing measurements are being carried out at LaRC's Chemistry And Physics of the Atmospheric Boundary Layer Experiment site (CAPABLE http://capable.larc.nasa.gov, 37.10°, −76.39°) in Hampton, VA, which is a moderately-urbanized area with regional NO_x emissions on the order of 0.1 Tg/year (based on a 2005 generated National Emission Inventory). CAPABLE is co-located with one of three Virginia Department of Environmental Quality's (VADEQ) Hampton Roads air-quality monitoring sites. The site can be considered as a coastal suburban site on the NW outer edge of the larger metropolitan area of Norfolk-Virginia Beach, but is considered part of the Virginia Beach-Norfolk-Newport News Metropolitan Statistical Area in the Mid-Atlantic region with a population in excess of one million. The site is subject to sporadic local and/or transported pollution events along with influences of sea-breeze effects from the southern part of the Chesapeake Bay as characterized by Martins et al. (2012). Nearby pollution sources are commuter traffic (including a service road 20 m south of the site and intermittent small-engine activity), an incinerator (0.5 km WSW), Yorktown Power Station (10 km NNW), the Newport News/Williamsburg airport (10 km NW), and Langley Air Force Base (1 km SE). In 2010, the four highest 8-hr maximum O_3 events measured at the site were 86 ppb on 06 July, 91 ppb on 07 July, 97 ppb on 11 August, and 78 ppb on 31 August. The most-recent 3-year average of 4th-highest O_3 days (2008–2010) is 74 ppb. All data available for the respective seasons were used to construct summer and winter diurnal NO_2 and O_3 profiles for this location and can be seen in Fig. 1(a, b).

2.2 Padonia & Edgewood, MD

Measurements at the Padonia (39.46°, −76.63°; 20 km N of Baltimore) and Edgewood (39.41°, −76.30°; 30 km NE of Baltimore) sites were made as part of the July-2011

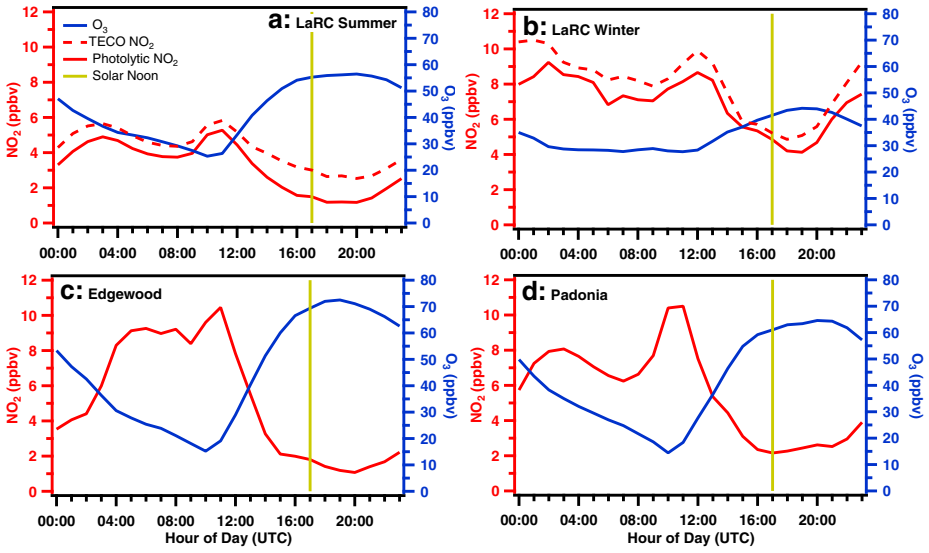

Fig. 1 Diurnal-mean plots for NO_2 and O_3 at the three locations studied

DISCOVER-AQ campaign, and act as case studies for exporting the methodology to sites that experience urban-level pollution (more in-depth case-study analyses from these sites will follow in subsequent publications), with the dominant pollution source being the Baltimore metropolitan area. Both sites were collocated with Maryland Department of the Environment (MDE) sites. Diurnal profiles for these locations are presented in Fig. 1(c, d). Similar to the CAPABLE site, due to Edgewood's proximity to the Chesapeake Bay a sea-breeze effect is commonly observed (Stauffer et al. 2012, *this issue*).

3 Instrumentation and comparison of PBL sources

3.1 NO_2 instrumentation

The current federal reference method (FRM) instrument for NO_2 (TECO 49C) uses a molybdenum-oxide converter with NO detected via chemiluminescence after reaction with O_3. This method also partially converts other oxides of nitrogen (collectively referred to as NO_z) such as nitric acid, alkyl nitrates, and peroxyacetyl nitrate to NO, leading to potentially false-high NO_2 readings (Dunlea et al. 2007; Grosjean and Harrison 1985; Steinbacher et al. 2007; Winer et al. 1974). Teledyne API 200EU monitors (limit of detection: 0.4 ppb, precision: 0.5 %) that utilize an LED-based photolytic converter followed by chemiluminescence for NO detection, effectively eliminating NO_z interference (Steinbacher et al. 2007), were located at the three sites in the current study, with a TECO 49C collocated at CAPABLE. Though photolytic-converter based NO_x instruments are not impervious to interference (e.g. HONO and photo-labile organic compounds, Sadanaga et al. 2010; Villena et al. 2012), none of the locations of the current study contained conditions appropriate to produce substantial amounts of NO_z (Elshorbany et al. 2010; Amoroso et al. 2008; Calvert et al. 1994). Mixing ratios of these interfering compounds are typically small (with the NO_x/NO_z ratio consistently heavily favoring NO_x), and are considered negligible in the current study. In the following analysis the API instrument was chosen over the current FRM instrument due to its highly-selective photolytic conversion of NO_2 to NO.

The ground-based spectrometer system (Pandora, vertical column density (VCD) precision: $\sim 3\times10^{14}$ mol.cm^{-2}) used in the current study has been validated against similar sun-tracking instruments (Wang et al. 2010), MAX-DOAS and zenith-looking instruments (Roscoe et al. 2010; Piters et al. 2012), and OMI (Herman et al. 2009). Pandora provides NO_2 VCDs from direct-sun observations that serve as a proxy for satellite-derived observations, such as OMI, with 90 s resolution, thereby allowing direct comparison of in-situ/column observations throughout the day as boundary-layer dynamics, emissions, and chemistry change. Sun-tracking instruments have the advantage over current MAX-DOAS instruments due to the substantially greater incoming signal, which significantly reduces integration time and dependence of the air-mass factor on parameters such as aerosol optical depth and surface albedo. However, they suffer disadvantages, as compared to active DOAS methods, in that they work only during daytime when the sun is visible.

OMI data (Goddard product, Boersma et al. 2001) were retrieved from the Goddard repository, and are used in the current analysis for all locations.

3.2 EDAS40 PBL

Planetary boundary layer data were acquired from the Eta Data Assimilation System model (EDAS40), which is produced by The National Weather Service's National Centers for

Environmental Prediction every 3 h. The EDAS40 model provides 40 km resolution, with 26 pressure surfaces, and estimates the PBL depth from the first inversion in the temperature profile. EDAS40 was chosen for its spatial resolution and availability to the community. These data were interpolated to provide 1-min resolution to properly account for the

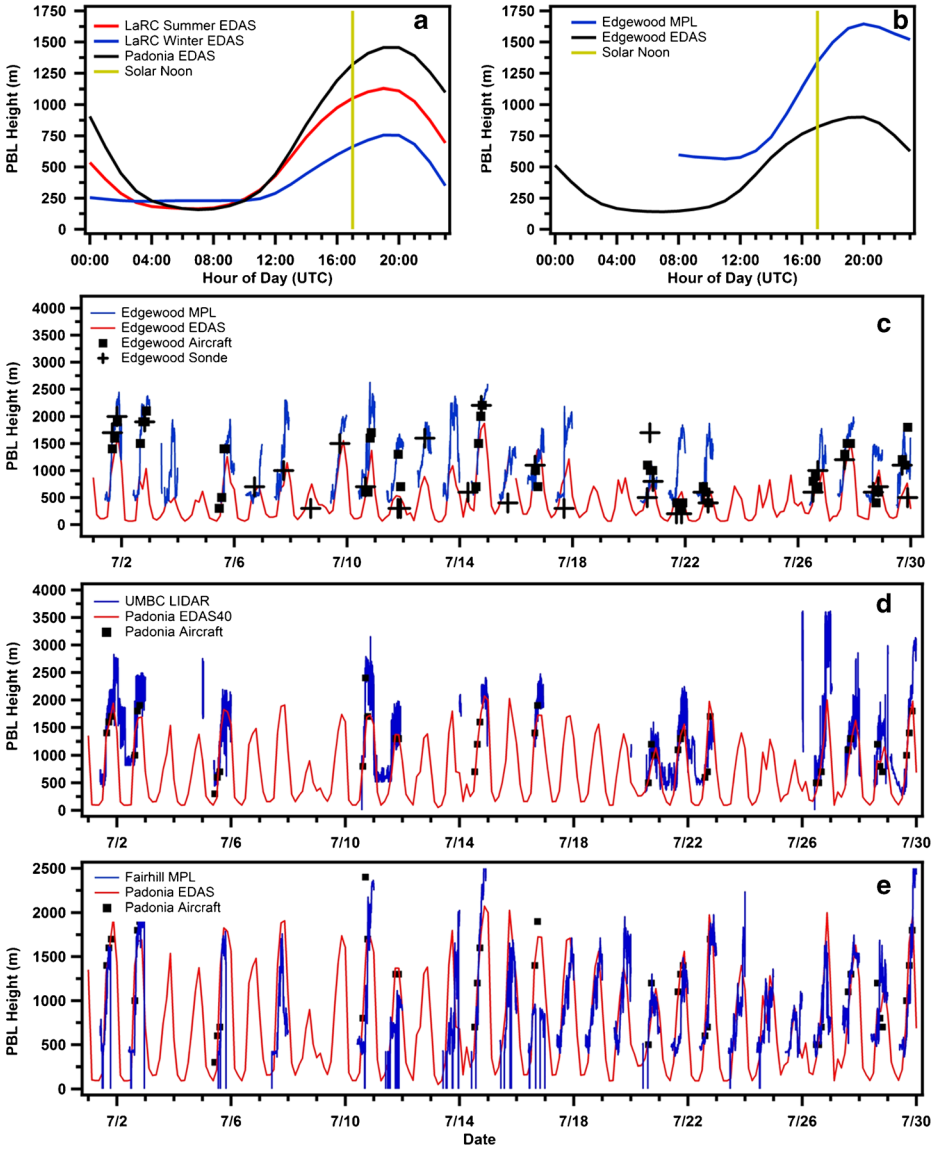

Fig. 2 Diurnal-mean profiles of EDAS40 PBL height at LaRC and Padonia (**a**), Edgewood (**b**), and the month of July 2011 for Edgewood (**c**), Padonia/UMBC (proximal to Padonia) using ELF LIDAR (**d**), and Padonia/Fairhill using MPL (**e**). All dates are UTC

influence of PBL variability. Diurnal profiles can be seen in Fig. 2, panels A and B. The EDAS40 data were inter-compared with sonde, aircraft, and LIDAR-derived PBL data that were collected at the Edgewood site. The results of this intercomparison will be briefly discussed below.

Since PBL uncertainty is not a standard product for the EDAS40 model, the uncertainty is assumed to be constant at 35 % for the current analysis. A brief discussion of the impact of this uncertainty is presented in Section 4.1.

3.3 Radiosonde/aircraft PBL

A total of 15 ozonesondes were launched at the CAPABLE site from June 22–July 22, 2010 and 39 ozonesondes were launched in Edgewood, MD as part of the DISCOVER-AQ project between July 1–July 31, 2011. Each ozonesonde was equipped with an electrochemical concentration cell (ENSCI, Corp. Model 2Z) to detect ozone, a radiosonde (Vaisala, Inc., RS-80 in 2010 and InterMet Systems, Inc., iMet-1 in 2011) that recorded pressure, temperature, humidity, wind speed, wind direction, and a GPS receiver (iMet only) to report location and height. Potential temperature profiles were calculated using the radiosonde data. PBL heights were determined objectively by first down-sampling the potential temperature data by block averaging every 50 m in the vertical starting at the surface. A localized lapse rate at height z was calculated by subtracting the potential temperature at height z from the potential temperature at height $z + 50\ m$ and dividing by 50 m. The PBL height was defined as the height closest to the surface and above 200 m with a localized lapse rate exceeding 7 K km^{-1}.

As part of the 2011 DISCOVER-AQ field campaign meteorological data (e.g. temperature, pressure, and humidity) were collected during aircraft spirals flown over the measurement sites. These data were used to calculate PBL heights, analogous to sonde data.

3.4 MPL PBL

Elastic LIDAR observations at Edgewood were performed using a Sigma Space Mini Micropulse LIDAR (MiniMPL). The MiniMPL transmitter consists of a 532 nm (frequency-doubled Nd:YAG, 5 kHz, 3–4 μJ) LASER. The receiver (80 mm telescope) focuses co-polarized backscattered light onto a photon counting silicon avalanche photo-diode (APD, Perkin-Elmer). The APD output is recorded by a field programmable gate array (FPGA) data system that enables display and storage of range dependent averaged count rates. Recorded LIDAR profiles have temporal and vertical resolution of 1 min and 30 m, respectively.

By using aerosols as tracers of atmospheric dynamics, LIDAR is a powerful tool for visualizing PBL aerosol content and dynamics in real time with high vertical resolution. The PBL typically contains greater aerosol concentration because the aerosols are trapped by a potential-temperature inversion. Therefore, the backscatter signal strength is greatly reduced when it transits from the PBL into the free troposphere. A covariance wavelet technique (CWT) was applied to the LIDAR signal to estimate these sharp gradient changes in backscatter profiles to determine the PBL height (Davis et al. 2000; Brooks 2003; Compton et al. 2012). The LIDAR-derived PBL diurnal cycle can be observed in Fig. 2b. Comparison and validation of the various PBL-estimation methods is outside the scope of the current

study, while analysis of how these various PBL methods influence the column-to-surface comparison remains the topic of this manuscript. However, to put the empirically-derived PBL values into perspective with the EDAS40 values, a brief comparison is presented below.

3.5 Comparison of PBL values

In the current analysis, EDAS40 PBL data were compared against three other PBL-determination methods (LIDAR, sonde, aircraft). Ratios of these values, with respect to EDAS40, are shown in Table 1 (perfect agreement yields a ratio of one). Ratios were calculated only for the Edgewood site since it was the only site to have a photolytic NO_2 monitor collocated with an MPL. It is observed that the mean ratio is best (closest to 1) for sonde and aircraft PBL values, though the coefficient of correlation is poor. Conversely, the mean ratio is smaller for the MPL comparison, but has a higher coefficient of correlation. The EDAS40 model characteristically under predicts the MPL-based PBL which, as discussed below, helps bring column observations (after conversion to mixing ratio values) into better agreement with surface measurements than do the MPL data. While this provides a comparison of the PBL methodologies used in the current study, this does not speak to how correct each method is in representing the actual PBL.

Figure 2(b–e) shows generally-poor quantitative agreement between the MPL and EDAS40-derived PBL heights for Edgewood, with moderate improvement for the other sites. Data from two additional DISCOVER-AQ sites (Fair Hill and University of Maryland Baltimore County (UMBC), MD) were used to expand the PBL comparison to include more inland sites. Indeed, sites that are further inland (e.g. Padonia and Fair Hill, panels D and E) appear to have better agreement, indicating the possibility that differences observed at Edgewood may be due to the complexities associated with marine–land interactions at that location. It was initially suspected that this disagreement may be due to the difference in temporal resolutions (EDAS40 model returning a PBL value every 3 h, vs. MPL every 1–2 min), despite the EDAS40 value being interpolated to one-minute resolution. This assumption was tested by performing three-hour averages on the MPL data, centered about the EDAS40 output times (e.g. 0000, 0300, 0600,…UTC), followed by interpolation to yield one-minute resolution data (effectively putting the three-hour MPL data through the same interpolation process as the EDAS40 data). As seen in Table 1, this averaging mechanism failed to bring the two data sets into significantly better agreement. Further discussion regarding these differences is offered below.

Table 1 Statistical comparison of EDAS40-derived PBL to other methodologies for data collected at Edgewood. Statistical data presented are based on ratio of EDAS40 and observed PBL values

	Mean	σ	Minimum	Maximum	R
EDAS40/MPL	0.64	0.28	0.11	2.02	0.73
EDAS40/$MPL_{EDAS\ RES}$	0.59	0.24	0.10	1.40	0.78
EDAS40/Sonde[a]	0.85	0.62	0.25	2.67	−0.10
EDAS40/Aircraft[a]	0.92	0.43	0.36	2.02	0.11

Data have been filtered to include only data points corresponding to SZA>75° unless otherwise noted

[a] Includes all data available, regardless of SZA. "EDAS RES" indicates 3-hour averaged MPL data that was then linearly interpolated to 1-minute resolution, identical to the processing of EDAS40 data; see Section 3.5

4 Methods

The PBL, defined as the layer that interacts with the surface on a time scale of hours, constitutes the lower-most layer of the atmosphere, and is the layer in which anthropogenic pollution is emitted, and often trapped under certain conditions. The height of the PBL is variable throughout the day (Fig. 2) as it responds to local surface heating, as well as other synoptic and mesoscale forcings. Differences in incoming solar radiation, which varies as a function of season, lead to higher PBL heights in summer than winter. Therefore, under well-mixed conditions and constant emission and removal rates, it would be reasonable to expect pollutant mixing ratios to vary inversely with PBL height while column density remains constant. Indeed, column variability appears to be independent of surface NO_2 mixing ratios until a PBL correction factor is applied, which brings the two data sets into relative harmony as seen in Fig. 3.

It has been well documented that NO_2 mixing ratios are often highly variable within the PBL (e.g. Halla et al. 2011; Piters et al. 2012; Sluis et al. 2010; Volten et al. 2009; Yang et al. 2010). However, the ability for making NO_2-profile measurements was not available throughout the entire measurement period; therefore, it is assumed here that surface emissions are well-mixed within the PBL as a first-order approximation (Leigh et al. 2007). The methodology for this surface estimation is presented below.

Total-column values were retrieved from the Pandora instrument with approximately 90 s resolution, and compared to surface values. Average in-situ NO_2 variability was very stable at all sites (average minute-to-minute change: ±0.08 ppb/min (σ=0.1 ppb/min), ±0.07 ppb/min (σ =.1 ppb/min), and ±0.1 ppb/min (σ=0.1 ppb/min) for LaRC, Edgewood, and Padonia respectively) except when impacted by local emissions (e.g. service road traffic and lawn mowers), which induced changes up to ±20 ppb/min. Therefore, all time series where $|\Delta NO_2| \geq$ 1.0 ppb/min were excluded from the analysis (<2 %, 2 %, and 3 % of the total for LaRC, Padonia, and Edgewood respectively). Pandora data were smoothed via a running-weighted

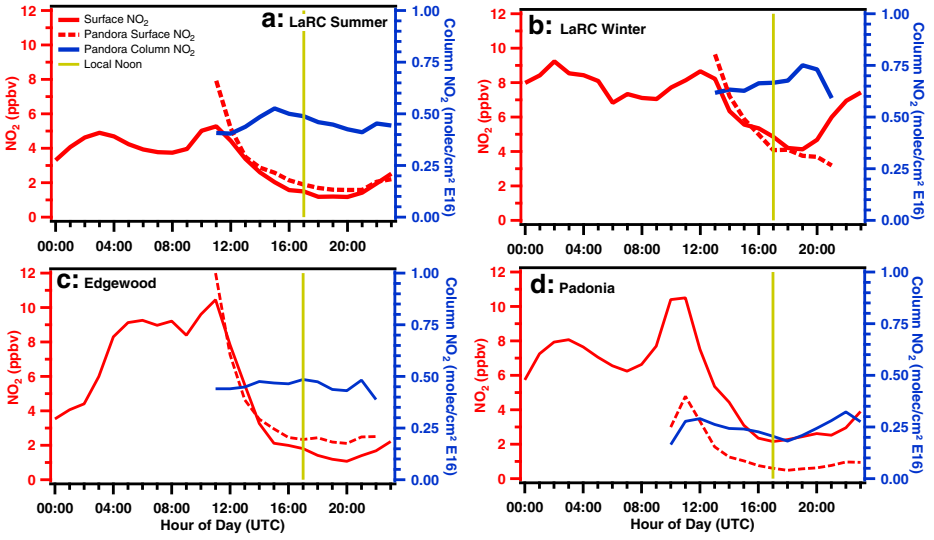

Fig. 3 Diurnal-mean plots for the three locations studied. Panels **a** and **b** contain data for LaRC during summer and winter respectively. Panels **c** and **d** contain only summer data (July 2011) collected at the Edgewood and Padonia sites, respectively. Pandora Surface NO_2 is the surface NO_2 estimated via the PBL-correction method of the tropospheric column

mean (weights: 0.025, 0.075, 0.150, 0.500, 0.150, 0.075, 0.025) to remove the short-term variability of atmospheric NO_2 while retaining the high temporal resolution of the measurement. This smoothing did not impact the basic findings of this analysis.

Daily OMI-derived stratospheric NO_2 (using the Goddard retrieval, Boersma et al. 2001; Bucsela et al. 2006) was subtracted from the Pandora-column observations from each site to yield tropospheric NO_2 column densities. On days when no OMI overpass data were available, the following day's value was used. This approximation is good, since the calculated day-to-day stratospheric variability is small (within 5×10^{14} mol.cm^{-2}, or ≈10 % of the total column under polluted conditions). Because of nitrogen dioxide's short photolytic lifetime outside the boundary layer, and temperature-dependent partitioning between NO_2 and NO, most of the tropospheric NO_2 column density resides in the PBL (Pisano et al. 1996; Sitnikov et al. 2005; Sluis et al. 2010; Fishman et al. 2011) and, under polluted conditions, the stratospheric contribution/variability is relatively minor throughout the day.

Pandora tropospheric NO_2 values were converted to mixing ratio values via Eq. (1) where $Pandora_{col}$ is the total column density measured by Pandora in molec/cm^2, OMI_{strat} is the stratospheric component as measured by OMI (free-tropospheric contribution is assumed to be negligible as in Lee et al. 2011), PBL is the boundary-layer height in centimeters, and N is the number density of air in molecules/cm^3. Although N is dependent on temperature and pressure, in addition to the fact that the temperature profile is variable within the PBL, we assume a constant T=290 K for these calculations. The utility and results from this initial approach are presented in Section 5.

$$C(\pm e_{tot}) = \frac{Pandora_{col}(\pm e_{pan}) - OMI_{strat}(\pm e_{omi})}{PBL(\pm e_{pbl}) * N} \quad (1)$$

4.1 Error analysis

The Pandora-based surface NO_2 error was estimated by propagating the uncertainty of the two measured values (OMI_{strat} (constant 2E14 molec/cm^2) and Pandora column NO_2 (calculated on point-by-point basis)) and applying a constant conservative uncertainty (35 %) to the EDAS40 PBL values since uncertainty is not a standard EDAS40 model product. We believe that ±35 % is an overestimate of the error, and will, therefore, provide a reasonable boundary. The median propagated uncertainty for each site is: 35 %, 35 %, and 36 % for LaRC, Edgewood, and Padonia respectively, indicative that PBL uncertainty is the dominant source of uncertainty in the estimation. Comparison of these uncertainties with the median percent differences confirms the assumed EDAS40 error to be overly conservative (Section 5).

Though the overall uncertainty is small, there are cases where the differences between in-situ and Pandora-derived surface NO_2 are significant, and vary on a site-by-site basis. This can be seen in the correlation plots in Fig. 4 wherein Pandora-based surface NO_2 estimates are plotted against a photolytic-converter based NO_x analyzer, and in the histogram plots (Fig. 5). While the agreement between the two methods tends to be good, accounting for these differences (i.e. spread in the data) will require further analysis including NO_2 vertical structure and meteorological conditions, and will be the subject of a future study.

A source of uncertainty that is not accounted for is sampling of different air masses by the in-situ and Pandora instruments due to the Pandora viewing geometry. As the sun rises (i.e. solar-zenith and azimuth angles change), and the PBL depth changes, Pandora's

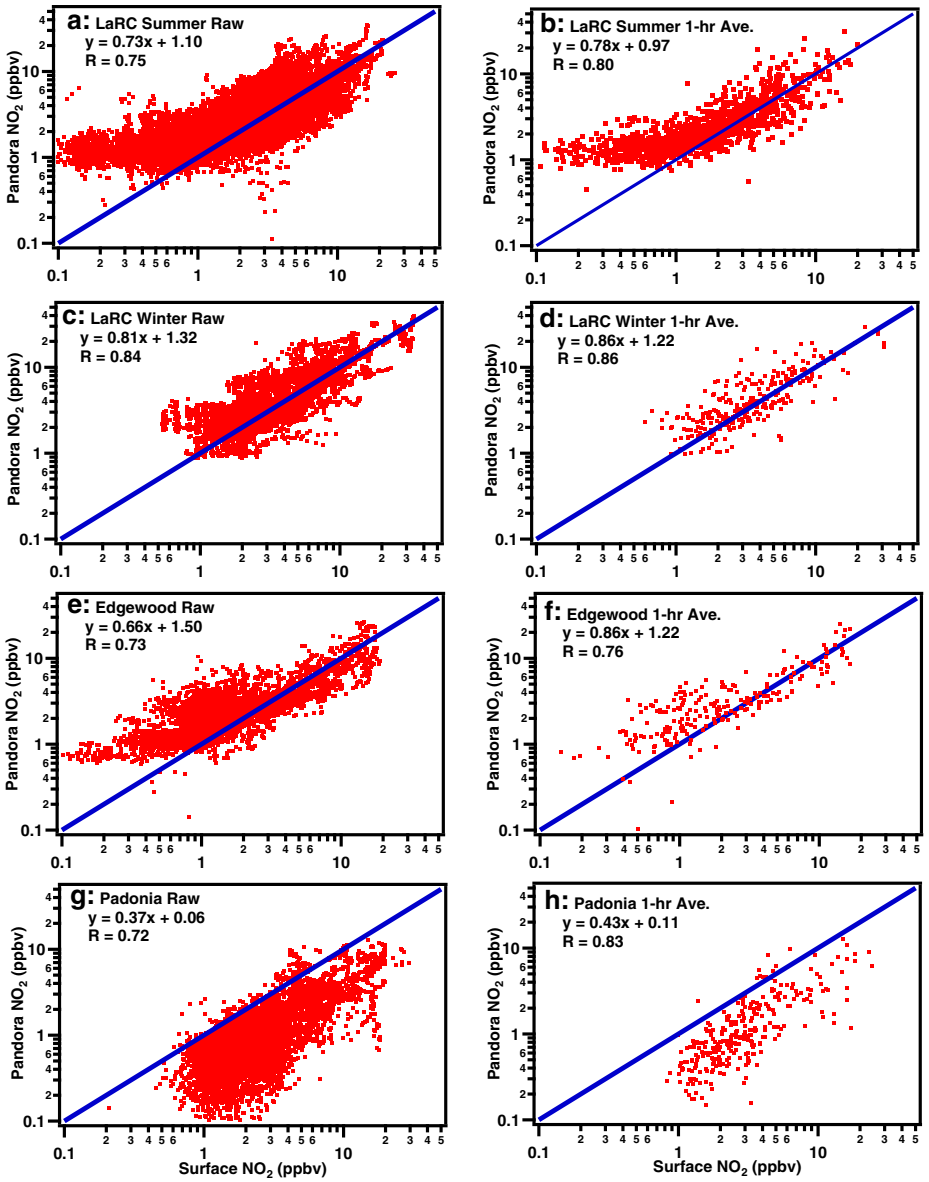

Fig. 4 Correlation plots for the three sites using differing temporal resolutions. Panels **a**, **c, e, g** have approximately 90 s resolution, while panels **b, d, f, h** have been averaged to one-hour resolution for CAPABLE, Edgewood, and Padonia sites respectively. *Blue line* is 1:1

observational path length within the PBL will consequently change. Therefore, it may be possible for Pandora to observe changes in NO_2 before or after the in-situ instrument, depending on wind direction and viewing geometry, and would show up in the data as a temporal offset between the two data sets. Though such discrepancies between the two instruments were not problematic in the current data sets (e.g. see Fig. 6, discussed below),

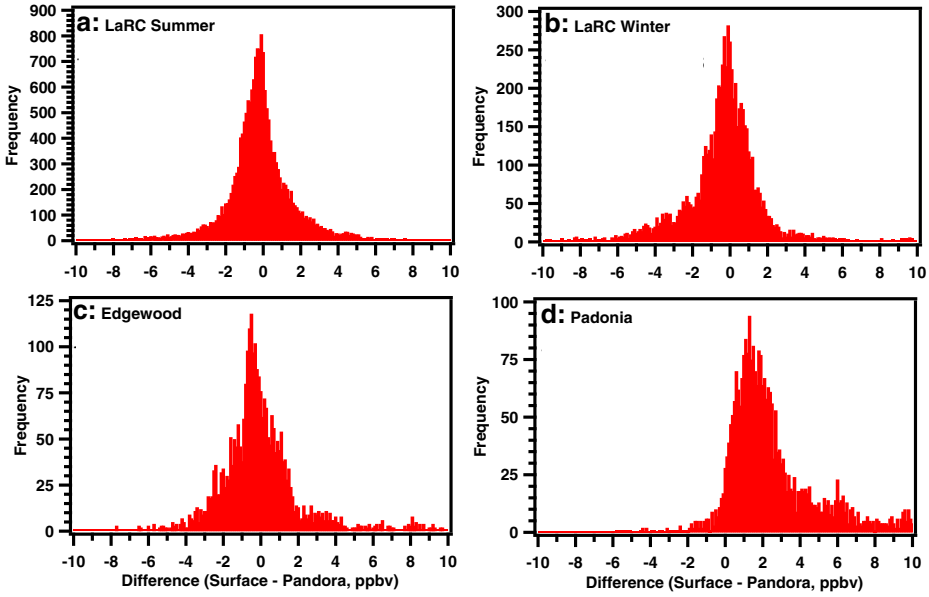

Fig. 5 Histogram plots of the difference between the Pandora-derived boundary-layer NO_2 mixing ratio and surface NO_2. Data sets have been limited to values with $NO_2 > 1$ ppb, and have approximately 90 s resolution

the potential for such effects should be noted. As this was not observed to be problematic in the current data set, this potential source of error is neglected in the current analysis.

5 Results and discussion

The data shown in Fig. 6 illustrate the qualitative agreement between the Pandora and in-situ instruments for the three locations studied, with the LaRC data set providing data from summer and winter seasons. Much of the temporal variability, on the order of 90 s to a few hours, is captured by both measurement techniques regardless of season or location, indicating the Pandora's ability to detect short time-scale boundary-layer NO_2 variations. It was observed that the direct-sun and surface NO_2 observations are in qualitative agreement on a day-to-day basis, particularly during elevated NO_2 events, and near solar noon. However, during high-zenith angle observations (i.e. low elevation angle) the Pandora-derived surface NO_2 was typically not in good agreement with the surface measurement (e.g. 12:00–13:00 UTC on 11-August, possibly due to a poorly developed PBL, poor representation of the PBL by the model, a residual layer, or horizontal variability), but improved by mid-morning as the PBL height grew from surface heating and buoyancy forces, leading to a well-mixed layer by this time. Consequently, data collected with a solar-zenith angle greater than 75° were neglected in the current analysis. In addition, early afternoon measurements frequently showed good quantitative agreement with OMI (Fig. 6 and discussion in Herman et al. 2009). As seen in Fig. 6, OMI tropospheric NO_2 data showed good agreement with surface values for the selected days after application of Eq. 1.

While the column and surface data are in general qualitative agreement (Fig. 6), there exist times when surface values change and the column remains constant (e.g. Fig. 6b from

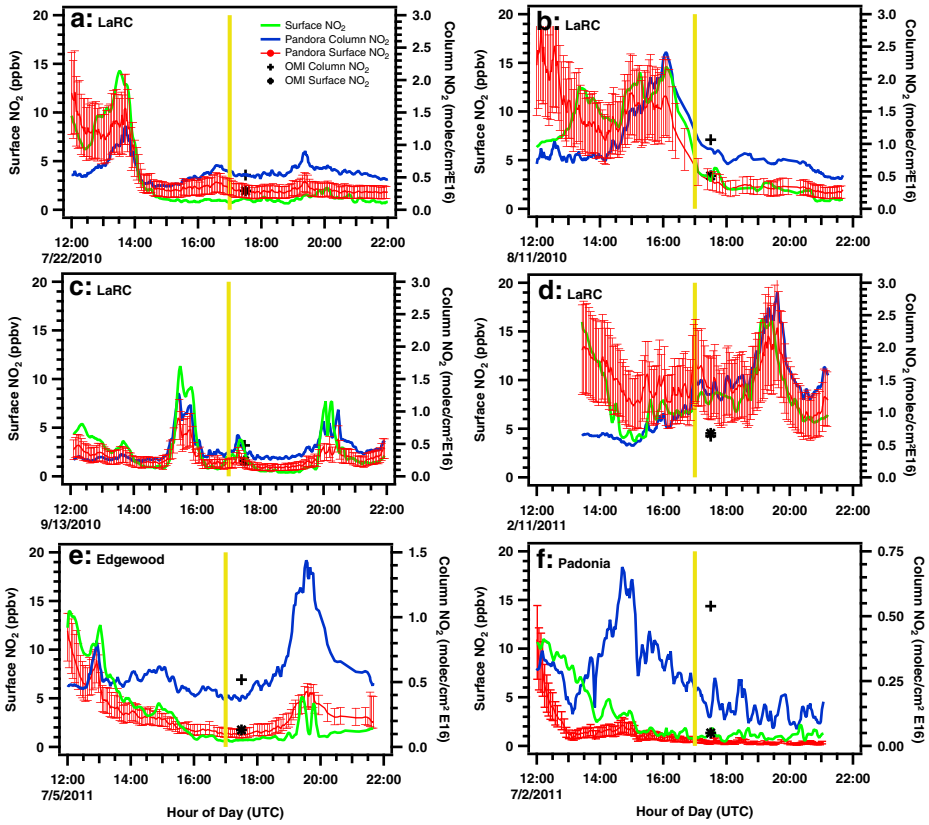

Fig. 6 Coincident plots of Pandora, API, and OMI NO_2 case-study days demonstrating Pandora's ability to observe boundary-layer NO_2 fluctuations. OMI VCD values are from the Goddard standard product, while the surface estimation was performed using the same methodology as the Pandora data for intercomparison. Notice change in VCD scales between LaRC and MD sites. *Gold bar* represents solar noon

12:00 to 14:00), or the two data sets seem to be inversely correlated (Fig. 3, panel b). Such disagreement is likely driven by PBL variability as application of a PBL-correction factor for estimation of surface NO_2 tends to bring the surface and column data sets into better agreement on time scales previously not recorded (i.e. minute resolution as opposed to monthly; Fig. 6). Indeed, previous studies have made monthly and seasonal comparisons between column and surface observations. Despite the inherent limitations of directly comparing these two observations (i.e. molec/cm^2 vs. parts per billion), when averaged over long time periods the two seem to correlate well (Kramer et al. 2008). Tables 2 and 3 present a correlation and regression analysis for the three sites studied. Data in Table 2 represent comparison of surface (ppb) and column (molec/cm^2) values, while Table 3 represents the same analysis after conversion of column data to an estimated surface value. It was observed that the column/surface comparison exhibited strong correlation (e.g. $R \approx 0.80$, not shown) when comparing week-long averaged values. However, the agreement broke down when comparing time frames that are more relevant to air-quality, health-impact, and emission inventory studies (e.g. minutes or hours). Conversion of column values to mixing ratio improved the correlation by, on average, an additional 40 percentage points (σ = ten percentage points; i.e. difference in R^2 values calculated from R in Tables 2 and 3), and a

Table 2 Statistical data for comparison of surface and column data prior to application of the EDAS40-derived PBL-correction factor

Location: average time	*R*	Slope (molec/cm^2 E16/ppb)	Intercept (molec/cm^2 E16)	Surface mean (ppb)
LaRC summer: raw	0.55	0.04	0.36	2.24
1-hr	0.61	0.04	0.35	2.25
LaRC winter: raw	0.49	0.03	0.51	4.57
1-hr	0.51	0.03	0.52	4.77
Edgewood: raw	0.48	0.03	0.38	2.80
1-hr	0.48	0.03	0.38	2.54
Padonia: raw	0.33	0.02	0.19	3.55
1-hr	0.31	0.02	0.21	3.45
LaRC summer >1 ppb: raw	0.46	0.04	0.39	3.37
1-hr	0.50	0.04	0.39	3.39
LaRC winter >1 ppb: raw	0.47	0.03	0.52	4.77
1-hr	0.49	0.03	0.53	4.87
Edgewood >1 ppb: raw	0.41	0.03	0.42	4.05
1-hr	0.45	0.03	0.43	3.85
Padonia >1 ppb: raw	0.32	0.02	0.20	3.69
1-hr	0.29	0.01	0.22	3.63

Hour-average data include only hours that contain 20 data points or more (maximum possible: 39) to limit uneven weighting. The tropospheric NO_2 column (molec/cm^2 E16) from Pandora was regressed on the surface-based measurements using a linear model

maximum of 60 percentage points. This improvement in correlation is statistically significant at the 99 % confidence level according to the z-test.

Correlation plots were constructed for the three sites, with summer and winter seasons separated for the LaRC data set (Fig. 4). Both LaRC and Edgewood sites experienced background NO_2 conditions ($NO_2 < 1$ ppb), while Padonia appeared to be more consistently polluted. It appears that Pandora's retrieval technique lost sensitivity to boundary-layer NO_2 when the NO_2 mixing ratio fell below ≈1 ppb. At such low mixing ratios, stratospheric variability becomes significant. Future studies need to be conducted so that stratospheric content and variability is better understood and eventually incorporated into Pandora or similar ground-based spectroscopic measurements. Due to this instrumental limitation, and the limited applicability of background NO_2 amounts for air-quality studies where the focus is on elevated trace gas concentrations, the remainder of the analysis was conducted only when NO_2 values (both surface and Pandora-derived) were above 1 ppb. The influence of this criterion on the resultant regression and correlation calculations is readily seen in Tables 2 and 3.

Distributions of the difference between the two instruments (surface–Pandora) can be seen in Fig. 5. These differences have narrow, normal distributions, approximately centered about zero (see Table 3 for details), for LaRC and Edgewood, while Padonia has a significant positive bias; potentially indicative of a shallow NO_2 scale height for this site, as previously observed at other sites (Petritoli et al. 2004). A key difference between the LaRC/Edgewood and Padonia sites is proximity to the bay, which may

Table 3 Similar to Table 2, but after application of the EDAS40-derived PBL-correction factor

Location: average time	*R*	Slope (ppb/ppb)	Intercept (ppb)	Surface mean (ppb)	Median bias (ppb)	Bias variability (1σ, ppb)
LaRC summer: raw	0.75	0.73	1.10	2.24	−0.62 (28 %)	1.79
1-hr	0.80	0.78	0.97	2.25	−0.54 (24 %)	1.50
LaRC winter: raw	0.84	0.81	1.32	4.57	−0.31 (7 %)	2.68
1-hr	0.86	0.86	1.22	4.77	−0.33 (7 %)	2.49
Edgewood: raw	0.73	0.66	1.50	2.80	−0.59 (21 %)	2.44
1-hr	0.76	0.57	1.60	2.54	−0.57 (22 %)	1.93
Padonia: raw	0.72	0.37	0.06	3.55	1.50 (42 %)	2.45
1-hr	0.83	0.43	0.11	3.45	1.50 (43 %)	1.94
LaRC summer >1 ppb: raw	0.69	0.71	1.27	3.38	−0.28 (8 %)	2.26
1-hr	0.74	0.76	1.13	3.45	−0.26 (8 %)	1.94
LaRC winter >1 ppb: raw	0.84	0.81	1.33	4.80	−0.26 (5 %)	2.75
1-hr	0.86	0.86	1.22	4.89	−0.29 (6 %)	2.56
Edgewood >1 ppb: raw	0.78	0.67	1.44	4.09	−0.36 (9 %)	2.42
1-hr	0.82	0.56	1.68	3.88	−0.28 (7 %)	1.98
Padonia >1 ppb: raw	0.68	0.31	0.94	5.56	1.90 (34 %)	3.27
1-hr	0.79	0.36	0.68	5.73	1.96 (34 %)	2.70

Differences between surface means for NO_2>1 ppb for Tables 2 and 3 are due to exclusion of data points corresponding to Pandora NO_2 being less than 1 ppb. Values in parentheses are indicative of percent difference (i.e. bias/surface mean). Here, bias is defined as surface minus Pandora NO_2 (ppb), which is represented graphically, for the entire data set, in Fig. 5

influence local chemistry and meteorology (Martins et al. 2012). As an example, Edgewood data were separated into bay-breeze and non-bay-breeze days where it is observed that most background NO_2 was observed during non-bay-breeze days (Fig. 7).

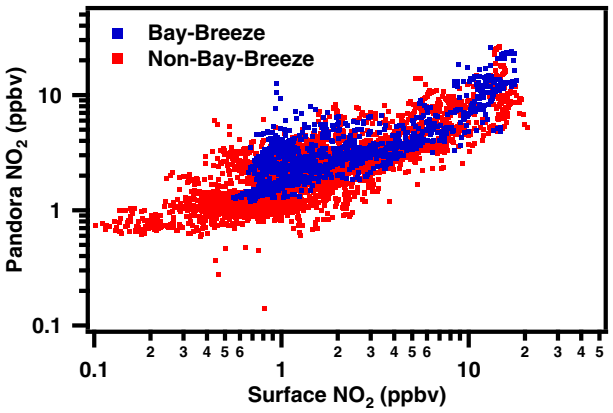

Fig. 7 Comparison of bay-breeze and non-bay-breeze days during the DISCOVER-AQ July 2011 field campaign for Edgewood, MD

Agreement between the column-based surface NO_2 estimation and the surface measurement at the three sites, which cover moderately-polluted and polluted environments, supports the hypothesis that an accurate knowledge of the PBL depth is an important factor that connects Pandora-column measurements with surface mixing ratios. Specifically, our findings indicate the EDAS40-derived PBL correction factor accounts for ≈50–75 % (R^2, Table 3) of the variability, with measurement frequency on the order of 90 s, thereby regaining high-temporal frequency information that is characteristically lost by satellite-based observations of only 1/day. As shown in Fig. 4 and Table 3, this methodology is also valid for 1-hour average values, which is important from a GEO-CAPE perspective as the GEO-CAPE mission is currently planned to achieve hourly coverage of the continental United States (Fishman et al. 2012). This may provide an important link in transitioning from a sparse network of surface-based monitors to continental coverage from a satellite-based instrument. Data presented in Figs. 4 and 6 and Table 3 are encouraging as implementation of one correction factor (PBL height), which is only an initial step of a larger problem, accounts for a significant amount of variability between the data sets.

5.1 Application of other PBL methods

PBL values were derived via three additional methods at the Edgewood, MD site during the 2011 DISCOVER-AQ field campaign, consisting of: LIDAR, sonde, and aircraft-spiral data. The MPL instrument yielded the largest, highest temporal resolution, PBL data set for the whole campaign, and will therefore be the most applicable to the current analysis.

It was observed that the MPL PBL values typically differed from the EDAS40 PBL (Figs. 2 and 8, Table 1), with the EDAS40 under representing the MPL value. Figure 9 shows side-by-side comparisons of the EDAS40-derived surface estimation (panels A and C), and surface-estimated NO_2 calculated using three additional methodologies (panels B and D) for 2 days at Edgewood. Here it is observed that when empirically-derived PBL values are used, estimation of surface NO_2 is characteristically underestimated as expected from Fig. 8. Figure 10 shows correlation plots for the MPL, sonde, and aircraft-derived surface NO_2 estimations, similar to Fig. 4, with regression statistics presented in Table 4, where it is observed again that surface NO_2 is being under-predicted (see slope values in Table 4).

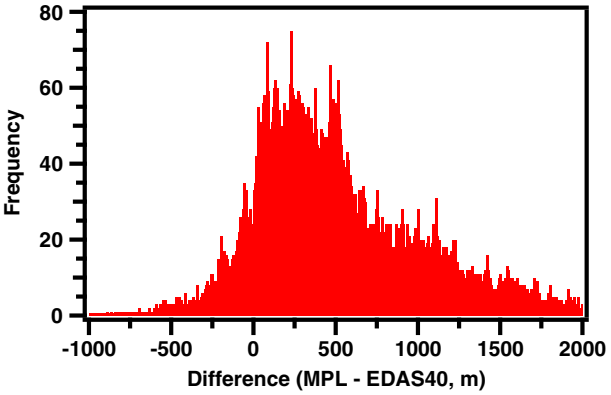

Fig. 8 Comparison of MPL and EDAS40-derived PBL values at the Edgewood site. Bin width of 1 m was used

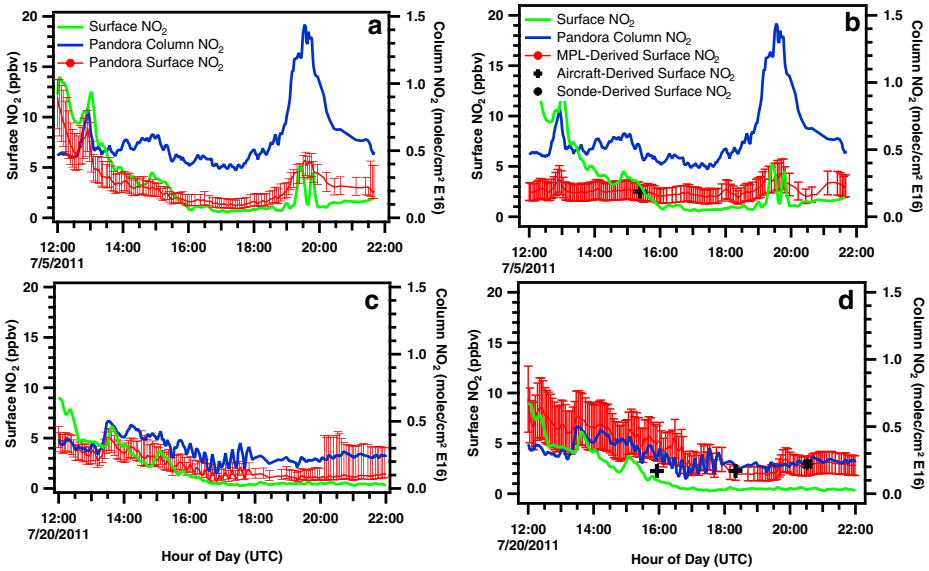

Fig. 9 Coincident plots for comparison of surface NO_2 estimation. Panels **a** and **c** display surface estimations using EDAS40 (same as in Fig. 6, presented here for side-by-side comparison), panels **b** and **d** present estimations incorporating MPL, sonde, and aircraft data

We find that empirically-derived PBL heights do not perform as well as modeled values that are reported on a three-hour basis with 40 km resolution (comparing R and bias values in Tables 3 and 4, Figs. 9 and 10), which is surprising, even though the methodology for determining PBL height for both the sonde and aircraft data is the same as that used for the EDAS40 model (i.e. temperature inversion). Good agreement between the aircraft/sonde and model-derived quantities can be partially explained by the relatively few coincident points (due to limited coincident observations) between the data sets. Conversely, the MPL instrument provided nearly continuous PBL values, with temporal resolution on the order of 1–2 min. Despite the higher temporal resolution of the MPL-derived PBL heights, the agreement between

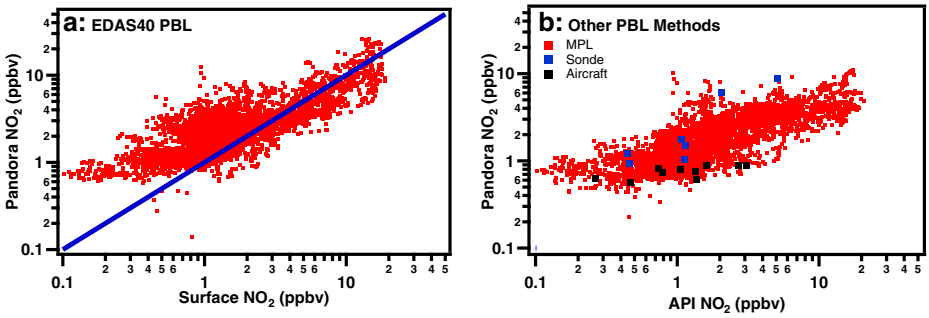

Fig. 10 Comparison of correlation plots for Edgewood data using the EDAS40 (**a**) and MPL, Sonde, and Aircraft-based PBL values (**b**). *Blue line* is 1:1

Table 4 Similar to Table 3, but with MPL, sonde, and aircraft PBL data used in the conversion, and only for the Edgewood site

PBL source: average time	R	Slope (ppb/ppb)	Intercept (ppb)	Surface mean (ppb)	Median bias (ppb)	Bias error (1σ, ppb)
MPL: raw	0.71	0.30	1.26	2.88	−0.04	2.67
1-hr	0.75	0.31	1.22	2.60	−0.03	2.21
MPL >1 ppb: raw	0.67	0.25	1.66	3.54	−0.07	3.02
1-hr	0.72	0.26	1.63	3.26	−0.06	2.56
Sonde: raw[a]	0.42	0.61	2.08	1.58	−0.89	2.01
Aircraft: raw[a]	−0.09	−0.16	3.28	1.34	−1.08	1.98

[a] Data set contains 13 or fewer observations

MPL-derived surface NO_2 was not better than those derived via EDAS40, especially under high NO_2 conditions (e.g. Fig. 10) where the surface estimation levels off (i.e. slope of regression is less than when EDAS40 PBLs were used). An initial suspicion was that EDAS40 performed better than MPL due to its coarser temporal resolution, which would be more representative of general, long-term, atmospheric conditions. This assumption was tested by averaging the MPL data to three-hour resolution to coincide with EDAS40 observations, then performing a weighted interpolation between the data points to yield one-minute resolution (Table 1). The results of this test were not significantly different from those obtained with the raw MPL data.

A likely reason for the lack of good agreement between the EDAS40 and MPL-derived surface NO_2 may be that the two PBL methodologies predict different variables, each of which has limitations in estimating PBL depth. While the aerosol PBL does represent one estimate of boundary layer height, and may work well under optimal conditions, it is not necessarily representative of the NO_2 scale height, which experiences different sources, sinks, and removal rates than aerosols. During the 2011 DISCOVER-AQ mission, aircraft-based NO_2 data were collected while the aircraft was spiraling about ground sites, from which the NO_2 scale height (altitude where NO_2 mixing ratio decreased to <36.7 % (1/e) of the surface value) was estimated. Figure 11 shows aircraft spiral data collected on two separate days over Edgewood, MD. Here it is observed how the vertical structure of NO_2 and particulate scattering at 550 nm both differ (panel A) and agree (panel B) depending on current conditions, with a numerical comparison presented in Table 5. Panel A is likely a case with a residual or buffer layer overlying a 750 m deep PBL where the PBL has collapsed and the aerosol remains, since there is no removal mechanism. NO_2 is not so well conserved, and furthermore, the overlying air may have come from a different location than the PBL air. The Panel B PBL looks to be about 1.5 km deep, with NO_2 extending above the PBL, which is replenished with PBL air more rapidly than the previous case. Indeed, NO_2 often has a complicated structure that is not supportive of the well-mixed assumption taken with this study, nor does it characteristically follow an exponential decay, which would be represented well by the scale height. On the contrary, it is observed to have layers aloft throughout the day, and to generally not follow the same pattern of the aerosol profile. Not understanding the NO_2 vertical structure introduces limitations on the applicability of column-to-surface conversions. An appropriate analysis of this issue is outside the scope of the current methodology, and will be the focus of future studies.

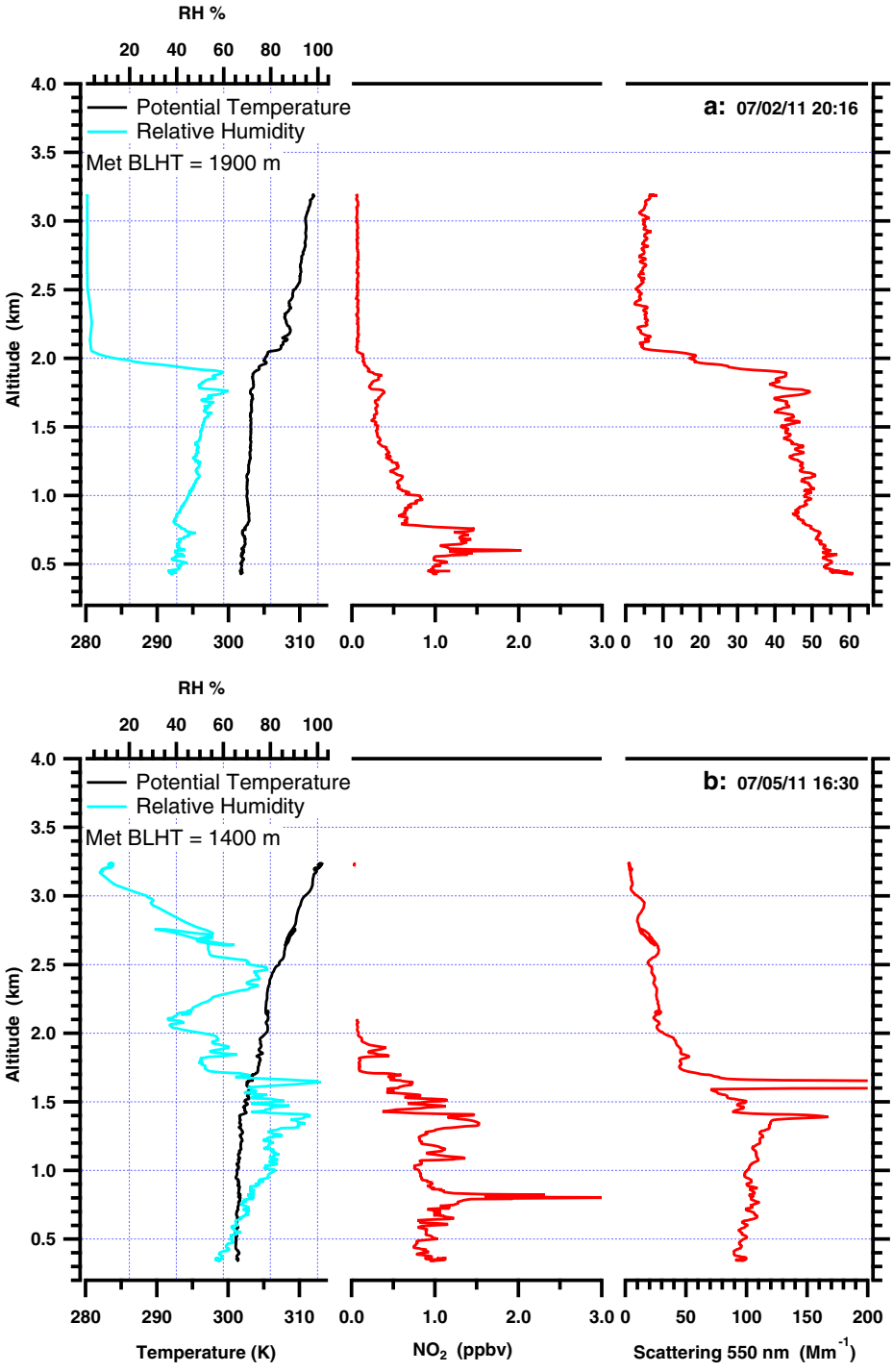

Fig. 11 Comparison of aircraft spiral data collected over Edgewood, MD. Panel **a** presents a case where the NO_2 scale height and aerosol-derived PBL values differ substantially, while Panel **b** presents a case where the two are in relative agreement. For numerical comparison with EDAS40, MPL, and meteorologically-defined PBL values see Table 5

Table 5 Comparison of PBL and scale-height values from two aircraft spirals. NO_2 scale height is estimated to be the first altitude where $[NO_2]_{aircraft} <= [NO_2]_{surf}*1/e$

Date/time (UTC)	NO_2 scale height (m)	550 nm scatter PBL (m)	EDAS40 PBL (m)	MPL PBL (m)	Met. PLB (m)
07/02/2011	750	2000	950	2000	1900
07/05/2011	1500	1500	1050	1450	1400

5.2 Application to SO_2

Applicability of this method to other atmospheric pollutants was tested for sulfur dioxide (SO_2) data collected at CAPABLE. SO_2 provides a significantly different set of conditions from NO_2 due to its longer atmospheric lifetime, differing sources, and vertical profile. The CAPABLE station frequently experienced elevated SO_2 levels due to its proximity to the Yorktown power station (≈10 km NNE, Fig. 12). As the wind shifted to NNE a spike in SO_2 and NO_2 is observed with corresponding O_3 titration, followed by dissipation to background conditions as the wind continued to come from a more easterly direction.

In contrast to NO_2, SO_2 over CAPABLE seemed to be more heterogeneously distributed throughout the atmosphere as seen by the poor agreement between the column and surface instruments (Figs. 13 and 14). When surface SO_2 was low, the Pandora instrument frequently detected significantly more SO_2 than did the surface instrument (R=0.18), indicative of non-negligible amounts of SO_2 existing above the boundary layer (example days plotted in Fig. 14). However, when the data set is

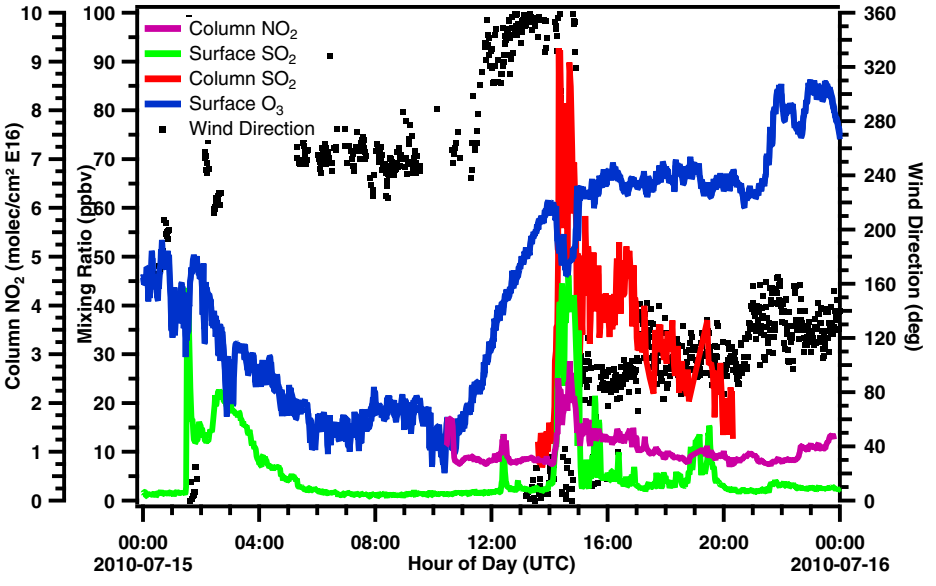

Fig. 12 Coincident plot of data collected during pollution transport from Yorktown power station showing that surface and column instruments located at CAPABLE are sensitive to point-source emissions

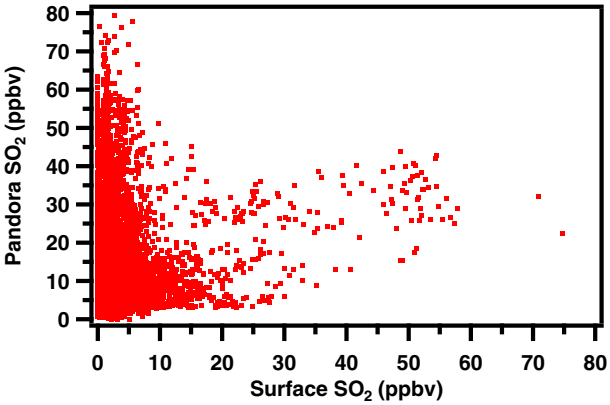

Fig. 13 Correlation plot of SO_2 data collected at CAPABLE

limited to only include values corresponding to elevated surface SO_2 (i.e. >10 ppb) the agreement significantly improved (R=0.70).

These results show that the Pandora instrument is capable of detecting rapid changes in local point-source emissions, and that the column NO_2 and SO_2 peaks occur simultaneously with a rapid drop in O_3 indicative of NO titration. Similar events were observed throughout the 2010 summer. However, in the current state of SO_2 analysis (i.e. requiring a surface measurement to filter background SO_2 data) applicability is limited to potentially identifying SO_2 layers aloft. Extended analysis of these events is outside the scope of the current manuscript, and will be the subject of future studies.

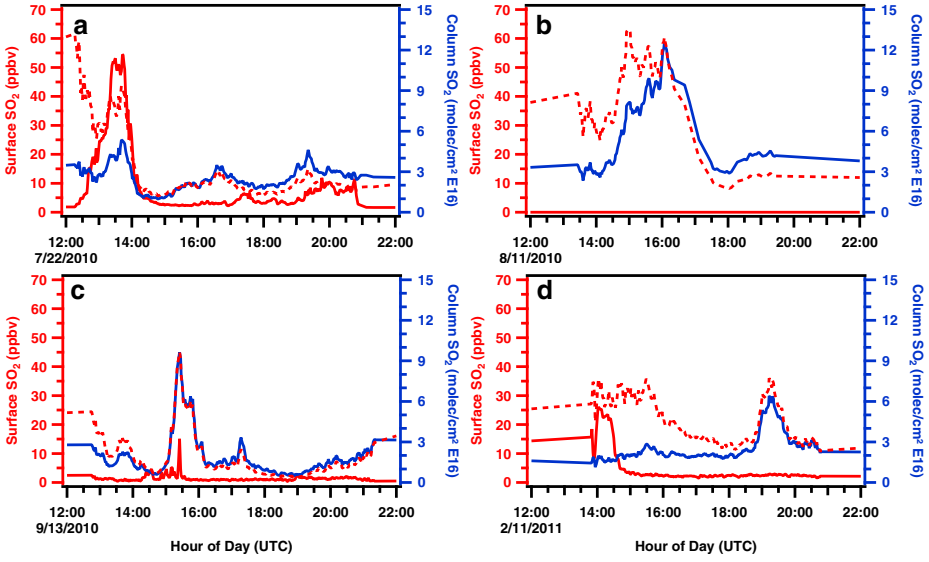

Fig. 14 Example coincident plots for SO_2 as measured at the CAPABLE site wherein it is observed that during background SO_2 conditions the agreement between surface-based and column observations is poor. During 11-August 2010 (**b**) no surface SO_2 data were available

6 Summary

This analysis shows the correlation between surface NO_2 and column observations supporting the initial assumption that daytime tropospheric NO_2 is predominantly located within the PBL (Pisano et al. 1996; Sitnikov et al. 2005; Sluis et al. 2010), that, to first order, column observations can be used for estimating surface NO_2 mixing ratios at the locations studied, and that information content in temporally-short observations may be significant enough to detect surface variability from geostationary space-based instruments (e.g. GEO-CAPE) with continental coverage.

The methodology presented shows encouraging agreement between column-converted and surface NO_2 data with high temporal resolution (i.e. 90 s and 1-hr averages) over the period July 2010–October 2011 at the CAPABLE site, and July 2011 for the DISCOVER-AQ work in the Baltimore area with incorporation of only one correction factor (i.e. model-derived PBL depth). Column data collected with a Pandora sun-tracking instrument were converted to a surface estimation value using the EDAS40 PBL, and were compared to the surface record from a photolytic-converter-based instrument for three different sites. The correlation between these two instruments was high (typically $R>0.75$), indicating that this method accounted for a significant fraction of the variability between the two techniques. The EDAS40 model was chosen due to its high spatial resolution and availability to the community at large. The methodology presented herein is applicable to both current and upcoming satellite missions (e.g. GEO-CAPE, TROPOMI), and ground-based-column-observing instruments that monitor tropospheric NO_2 levels with high temporal resolution. Due to the availability of the EDAS40 data set, similar techniques may be useful in converting satellite column values on a larger scale, though feasibility studies must be carried out to investigate how these products vary as a function of regional conditions.

Incorporating a PBL correction factor greatly improved agreement between surface/column observations, corroborating that tropospheric NO_2 resides predominantly in the PBL. Previous work has focused on significant temporal averaging (e.g. monthly, seasonal), which is useful for analyzing historical trends and studying climatologies. However, the data and methodology presented herein, with a 90 s resolution, will be useful in extending our capabilities from making historical observations to providing valuable insight into processes taking place on time scales of hours. Continued analysis of Pandora and surface NO_2 data will help define temporal characteristics of local NO_2 variability and how this relates to surface NO_2 mixing ratios (e.g. for acute health impacts), with the overall goal of applying similar methodologies to space-based observations. The ability to resolve these shorter time scale episodes with coverage only available via satellite observation will significantly further our understanding of boundary-layer chemistry, the evolution and transport of pollution events, as well as provide a significant step forward in the development of regional-scale chemical/transport models. As GEO-CAPE is currently planned to make hourly continental-U.S. observations, the results of this study, which show strong correlation for hourly-averaged data, may be applicable to this mission and elucidate the relationship between column and surface observations. A key conclusion of this study is that data collected from geostationary satellite instruments, which will provide hourly continental coverage (as opposed to a sparse in-situ network), and will not have long integration time on a point-by-point basis, may be able to detect short timescale surface fluctuations in NO_2 in both a qualitative and quantitative manner. It is these high-temporal resolution observations that are key from a health/air-quality perspective as mortality is significantly linked to high NO_2 events that may not be observed from current daily overpass data.

It was shown that the choice of PBL definition is critical when performing column-to-surface estimations. Application of aerosol-based PBL data was significantly worse than that

from the EDAS40 model, which is most likely due to differences between meteorological and chemical PBL/mixed-layer definitions.

SO_2 is a primary air-quality constituent that is detectable with Pandora systems and satellite-based instrumentation. This analysis shows that under elevated SO_2 conditions, the agreement between column-based surface estimation and surface conditions has an improved correlation. However, under background and moderate conditions the correlation drops significantly. This disagreement may be attributed to SO_2 aloft, and the differing sources and lifetimes of SO_2 and NO_2. Further analysis is required to understand this relationship.

Our results show that for large zenith angles, the correlation is poorer which may be the result of a less-well-mixed PBL, a poor PBL estimation from the model, or an overlying residual layer. Further exploration is required to understand this time of day dependence, how boundary-layer dynamics influence chemical mixing/distribution, and how this influences satellite retrievals. Application of this methodology to additional case studies from the 2011 DISCOVER-AQ mission, and current satellite retrieval data, will be the focus of future analyses.

Elucidation of NO_2 distribution throughout the PBL is the key to understanding how column observations relate to ground conditions, and applying the current methodology to satellite data sets. The methodology presented herein is a first step that shows promise in making satellite-based observations applicable to regulatory and emissions inventory work. Application of this methodology is limited to daytime observations (though ground-based moon-tracking instruments are available), and times when the PBL is well developed, which may be problematic for nocturnal observations. This technique also shows potential for application during high SO_2 events, which requires surface measurements for identification, and observation of SO_2 aloft. Indeed, future studies will focus on refining the SO_2 analysis, and improving our understanding of the meteorological drivers that influence the NO_2 correlations.

Acknowledgments Funding for this work was provided by NASA Applied Sciences Program, EPA collaborations under an EPA-LaRC memorandum of agreement, GEO-CAPE mission studies, and Langley Innovative Partnership Program. T. Knepp was supported through NASA's post-doctoral program. The National Center for Atmospheric Research is sponsored by the National Science Foundation. Although this paper has been reviewed by the EPA and approved for publication, it does not necessarily reflect EPA policies or views.

References

Amiot, N., Tillon, J., Viacroze, C., Aouine, H., Muir, J.F.: Consequences of atmospheric pollution fluctuations in patients with COPD. Rev. Fr. Allergol. (2012). doi:10.1016/j.reval.2010.10.002

Amoroso, A., Beine, H.J., Esposito, G., Perrino, C., Catrambone, M., Allegrini, I.: Seasonal differences in atmospheric nitrous acid near Mediterranean urban areas. Water Air Soil Pollut. (2008). doi:10.1007/s11270-007-9526-6

Andersen, Z.J., Kristiansen, L.C., Andersen, K.K., Olsen, T.S., Hvidberg, M., Jensen, S.S., Ketzel, M., Loft, S., Sorensen, M., Tjonneland, A., Overvad, K., Raaschou-Nielsen, O.: Stroke and long-term exposure to outdoor air pollution from nitrogen dioxide a cohort study. Stroke (2012). doi:10.1161/STROKEAHA.111.629246

Boersma, K.F., Bucsela, E.J., Brinksma, E.J., Gleason, J.G.: OMI-EOS algorithm theoretical basis document: Trace gas algorithms: NO_2. **4**, 12–35 (2001)

Boersma, K.F., Jacob, D.J., Trainic, M., Rudich, Y., DeSmedt, I., Dirksen, R., Eskes, H.J.: Validation of urban NO_2 concentrations and their diurnal and seasonal variations observed from the SCIAMACHY and OMI sensors using in situ surface measurements in Israeli cities. Atmos. Chem. Phys. **9**, 3867–3879 (2009)

Brooks, I.M.: Finding boundary layer top: Application of a wavelet covariance transform to lidar backscatter profiles. J. Atmos. Ocean. Technol. **20**, 1092–1105 (2003)

Brunekreef, B., Holgate, S.T.: Air pollution and health. Lancet **360**, 1233–1242 (2002)

Bucsela, E., Celarier, E., Wenig, M., Gleason, J., Veefkind, P., Boersma, K.F., Brinksma, E.: Algorithm for NO2 vertical column retrieval from the Ozone Monitoring Instrument. IEEE Trans. Geosci. Remote Sens. **44**, 1245–1258 (2006)

Calvert, J.G., Yarwood, G., Dunker, A.M.: An evaluation of the mechanism of nitrous-acid formation in the urban atmosphere. Res. Chem. Intermed. (1994). doi:10.1163/156856794X00423

Compton, J., Delgado, R., Berkoff, T., Hoff, R.: Determination of planetary boundary layer height on short spatial and temporal scales: A demonstration of the Covariance Wavelet Transform in ground based wind profiler and lidar measurements. J. Atmos. Oceanic Technol. (2013). doi:10.1175/JTECHD-12-00116.1

Davis, K.J., Gamage, N., Hagelberg, C.R., Kiemle, C., Lenschow, D.H., Sullivan, P.P.: An objective method for deriving atmospheric structure from airborne lidar observations. J. Atmos. Ocean. Technol. **17**, 1455–1468 (2000)

Dunlea, E.J., Herndon, S.C., Nelson, D.D., Volkamer, R.M., San Martini, F., Sheehy, P.M., Zahniser, M.S., Shorter, J.H., Wormhoudt, J.C., Lamb, B.K., Allwine, E.J., Gaffney, J.S., Marley, N.A., Grutter, M., Marquez, C., Blanco, S., Cardenas, B., Retama, A., Ramos Villegas, C.R., Kolb, C.E., Molina, L.T., Molina, M.J.: Evaluation of nitrogen dioxide chemiluminescence monitors in a polluted urban environment. Atmos. Chem. Phys. **7**, 2691–2704 (2007)

Elshorbany, Y., Barnes, I., Becker, K.H., Kleffmann, J., Wiesen, P.: Sources and cycling of tropospheric hydroxyl radicals—an overview. Int. J. Res. Phys. Chem. Chem. Phys. (2010). doi:10.1524/zpch.2010.6136

Fishman, J., Bowman, K.W., Burrows, J.P., Richter, A., Chance, K.V., Edwards, D.P., Martin, R.V., Morris, G.A., Pierce, R.B., Ziemke, J.R., Al-Saadi, J.A., Creilson, J.K., Schaack, T.K., Thompson, A.M.: Remote sensing of tropospheric pollution from space. Bull. Am. Meteorol. Soc. **89**, 805–821 (2008)

Fishman, J., Silverman, M.L., Crawford, J.H., Creilson, J.K.: A study of regional-scale variability of in-situ and model-generated tropospheric trace gases: Insights into observational requirements for a satellite in geostationary orbit. Atmos. Environ. (2011). doi:10.1016/j.atmosenv.2011.05.008

Fishman, J., Iraci, L.T., Al-Saadi, J., Bontempi, P., Chance, K., Chavez, F., Chin, M., Coble, P., Davis, C., DiGiacomo, P., Edwards, D., Eldering, A., Goes, J., Herman, J., Hu, C., Jacob, D., Jordan, C., Kawa, S.R., Key, R., Liu, X., Lohrenz, S., Mannino, A., Natraj, V., Neil, D., Neu, J., Newchurch, M., Pickering, K., Salisbury, J., Sosik, H., Subramaniam, A., Tzortziou, M., Wang, J., Wang, M.: The United States' next generation of atmospheric composition and coastal ecosystem measurements: NASA's Geostationary Coastal and Air Pollution Events (GEO-CAPE) mission. Bull. Am. Meteorol. Soc. **93**, 1547–1566 (2012)

Ghude, S.D., Van der A, R.J., Beig, G., Fadnavis, S., Polade, S.D.: Satellite derived trends in NO_2 over the major global hotspot regions during the past decade and their inter-comparison. Environ. Pollut. (2009). doi:10.1016/j.envpol.2009.01.013

Grosjean, D., Harrison, J.: Response of chemi-luminescence NOx analyzers and ultraviolet ozone analyzers to organic air-pollutants. Environ. Sci. Technol. **19**, 862–865 (1985)

Halla, J.D., Wagner, T., Beirle, S., Brook, J.R., Hayden, K.L., O'Brien, J.M., Ng, A., Majonis, D., Wenig, M.O., McLaren, R.: Determination of tropospheric vertical columns of NO_2 and aerosol optical properties in a rural setting using MAX-DOAS. Atmos. Chem. Phys. (2011). doi:10.5194/acp-11-12475-2011

Herman, J., Cede, A., Spinei, E., Mount, G., Tzortziou, M., Abuhassan, N.: NO2 column amounts from ground-based Pandora and MFDOAS spectrometers using the direct-sun DOAS technique: Intercomparisons and application to OMI validation. J. Geophys. Res.-Atmos. (2009). doi:10.1029/2009JD011848

Irie, H., Boersma, K.F., Kanaya, Y., Takashima, H., Pan, X., Wang, Z.F.; Quantitative bias estimates for tropospheric NO2 columns retrieved from SCIAMACHY, OMI, and GOME-2 using a common standard for East Asia. Atmos. Meas. Tech. **5** (2012) doi:10.5194/amt-5-2403-2012

Koelemeijer, R.B.A., Homan, C.D., Matthijsen, J.: Comparison of spatial and temporal variations of aerosol optical thickness and particulate matter over Europe. Atmos. Environ. **40**, 5304–5315 (2006)

Kramer, L.J., Leigh, R.J., Remedios, J.J., Monks, P.S.: Comparison of OMI and ground-based in situ and MAX-DOAS measurements of tropospheric nitrogen dioxide in an urban area. J. Geophys. Res. (2008). doi:10.1029/2007JD009168

Krishna, M., Springall, D., Meng, Q.H., Withers, N., Macleod, D., Biscione, G., Frew, A., Polak, J., Holgate, S.: Effects of ozone on epithelium and sensory nerves in the bronchial mucosa of healthy humans. Am. J. Respir. Crit. Care **156**, 943–950 (1997)

Lamsal, L.N., Martin, R.V., van Donkelaar, A., Steinbacher, M., Celarier, E.A., Bucsela, E., Dunlea, E.J., Pinto, J.P.: Ground-level nitrogen dioxide concentrations inferred from the satellite-borne Ozone Monitoring Instrument. J. Geophys. Res.-Atmos. (2008). doi:10.1029/2007JD009235

Lamsal, L.N., Martin, R.V., van Donkelaar, A., Celarier, E.A., Bucsela, E.J., Boersma, K.F., Dirksen, R., Luo, C., Wang, Y.: Indirect validation of tropospheric nitrogen dioxide retrieved from the OMI satellite instrument: Insight into the seasonal variation of nitrogen oxides at northern midlatitudes. J. Geophys. Res. (2010). doi:10.1029/2009JD013351

Lee, C.J., Brook, J.R., Evans, G.J., Martin, R.V., Mihele, C.: Novel application of satellite and in-situ measurements to map surface-level NO_2 in the Great Lakes region. Atmos. Chem. Phys. (2011). doi:10.5194/acp-11-11761-2011

Leigh, R.J., Corlett, G.K., Frieß, U., Monks, P.S.: Spatially resolved measurements of nitrogen dioxide in an urban environment using concurrent multi-axis differential optical absorption spectroscopy. Atmos. Chem. Phys. **7**, 4751–4762 (2007)

Lin, X., Trainer, M., Liu, S.C.: On the nonlinearity of the tropospheric ozone production. J. Geophys. Res.-Atmos. (1988). doi:10.1029/JD093ID12p15879

Liu, S., Trainer, M., Fehsenfeld, F.C., Parrish, D.D., Williams, E.J., Fahey, D.W., Hubler, G., Murphey, P.C.: Ozone production in the rural troposphere and the implications for regional and global ozone distributions. J. Geophys. Res.-Atmos. (1987). doi:10.1029/JD092iD04p04191

Liu, L.J.S., Tsai, M.Y., Keidel, D., Gemperli, A., Ineichen, A., Hazenkamp-von Arx, M., Bayer-Oglesby, L., Rochat, T., Kunzli, N., Ackermann-Liebrich, U., Straehl, P., Schwartz, J., Schindler, C.: Long-term exposure models for traffic related NO(2) across geographically diverse areas over separate years. Atmos. Environ. (2012). doi:10.1016/j.atmosenv.2011.09.021

Luo, Y.H., Sun, L.G., Liu, W.Q., Xie, P.H., Si, F.Q., Zhou, H.J.: MAX-DOAS measurements of NO2 column densities and vertical distribution at Ny-Ålesund, Arctic during summer. Spectrosc. Spectr. Anal. (2012). doi:10.3964/j.issn.1000-0593(2012)09-2336-05

Maheswaran, R., Pearson, T., Smeeton, N.C., Beevers, S.D., Campbell, M.J., Wolfe, C.D.: Impact of outdoor air pollution on survival after stroke population-based cohort study. Stroke **41**, 869–877 (2010)

Martins, D.K., Stauffer, R.M., Thompson, A.M., Knepp, T.N., Pippin, M.: Surface ozone at a coastal suburban site in 2009 and 2010: Relationships to chemical and meteorological processes. J. Geophys. Res.-Atmos. (2012). doi:10.1029/2011JD016828

Meng, Z., Dabdub, D., Seinfeld, J.H.: Chemical coupling between atmospheric ozone and particulate matter. Science **277**, 116–119 (1997)

Noguchi, K., Itoh, H., Shibasaki, T., Hayashida, S., Uno, I., Ohara, T., Richter, A., Burrows, J.P.: Comparison of tropospheric NO2 observations by GOME and the air-quality monitoring network around Tokyo, Japan. J. Remote Sens. Soc. Jpn. **29**, 398–409 (2009)

Ordonez, C., Richter, A., Steinbacher, M., Zellweger, C., Nüß, H., Burrows, J.P., Prevot, A.S.H.: Comparison of 7 years of satellite-borne and ground-based tropospheric NO2 measurements around Milan, Italy. J. Geophys. Res.-Atmos. (2006). doi:10.1029/2005JD006305

Petritoli, A., Bonasoni, P., Giovanelli, G., Ravegnani, F., Kostadinov, I., Bortoli, D., Weiss, A., Schaub, D., Richter, A., Fortezza, F.: First comparison between ground-based and satellite-borne measurements of tropospheric nitrogen dioxide in the Po basin. J. Geophys. Res.-Atmos. (2004). doi:10.1029/2004JD004547

Pisano, J., Drummond, J., Hastie, D.R.: A lightweight NO2 instrument for vertical height profiles. J. Atmos. Ocean Technol. **13**, 400–406 (1996)

Piters, A.J.M., Boersma, K.F., Kroon, M., Hains, J.C., Van Roozendael, M., Wittrock, F., Abuhassan, N., Adams, C., Akrami, M., Allaart, A.F., Apituley, A., Beirle, S., Bergwerff, J.B., Berkhout, A.J.C., Brunner, D., Cede, A., Chong, J., Clemer, K., Fayt, C., Frieß, U., Gast, L.F.L., Gil-Ojeda, M., Goutail, F., Graves, R., Griesfeler, A., Großmann, K., Hemerijckx, G., Hendrick, F., Henzing, B., Herman, J., Hermans, C., Hoexum, M., van der Hoff, G.R., Irie, H., Johnston, P.V., Kanaya, Y., Kim, Y.J., Klein Baltink, H., Kreher, K., de Leeuw, G., Leigh, R., Merlaud, A., Moerman, M.M., Monks, P.S., Mount, G.H., Navarro-Comas, M., Oetjen, H., Pazmino, A., Perez-Camacho, M., Peters, E., du Piesanie, A., Pinardi, G., Puentedura, O., Richter, A., Roscoe, H.K., Schönhardt, A., Schwarzenbach, B., Shaiganfar, R., Sluis, W., Spinei, E., Stolk, A.P., Strong, K., Swart, D.P.J., Takashima, H., Vlemmix, T., Vrekoussis, M., Wagner, T., Whyte, C., Wilson, K.M., Yela, M., Yilmaz, S., Zieger, P., Zhou, Y.: The Cabauw intercomparison campaign for Nitrogen Dioxide measuring Instruments (CINDI): Design, execution, and early results. Atmos. Meas. Tech. (2012). doi:10.5194/amt-5-457-2012

Richter, A., Burrows, J., Nuss, H., Granier, C., Niemeier, U.: Increase in tropospheric nitrogen dioxide over China observed from space. Nature (2005). doi:10.1038/nature04092

Roscoe, H.K., Van Roozendael, M., Fayt, C., du Piesanie, A., Abuhassan, N., Cede, A., Chong, J., Clemer, K., Frieß, U., Ojeda, M.G., Goutail, F., Graves, R., Griesfeller, A., Grossmann, K., Hemerijckx, G., Hendrick, F.,

Herman, J., Hermans, C., Irie, H., Johnston, P.V., Kanaya, Y., Kreher, K., Leigh, R., Merlaud, A., Mount, G.H., Navarro, M., Oetjen, H., Pazmino, A., Perez-Camacho, M., Peters, E., Pinardi, G., Puentedura, O., Richter, A., Schönhardt, A., Shaiganfar, R., Spinei, E., Strong, K., Takashima, H., Vlemmix, T., Vrekoussis, M., Wagner, T., Wittrock, F., Yela, M., Yilmaz, S., Boersma, F., Hains, J., Kroon, M., Piters, A., Kim, Y.J.: Intercomparison of slant column measurements of NO2 and O4 by MaxDOAS and zenitz-sky UV and visible spectrometers. Atmos. Meas. Tech. (2010). doi:10.5194/amt-3-1629-2010

Sadanaga, Y., Fukumori, Y., Kobashi, T., Nagata, M., Takenaka, N., Bandow, H.: Development of a selective light-emitting diode photolytic NO2 converter for continuously measuring NO2 in the atmosphere. Anal. Chem. **82**, 9234–9239 (2010)

Schneider, P., van der A, R.J.: A global single-sensor analysis of 2002–2011 tropospheric nitrogen dioxide trends observed from space. J. Geophys. Res. Atmos. (2012). doi:10.1029/2012JD017571

Sitnikov, N.M., Sokolov, A.O., Ravegnani, F., Yushkov, V.A., Ulanovskiy, A.E.: A chemiluminescent balloon-type nitrogen dioxide meter for tropospheric and stratospheric investigations (NaDA). Phys. Instrum. Ecol. Med. Biol. **48**, 136–141 (2005)

Sluis, W.W., Allaart, M.A.F., Piters, A.J.M., Gast, L.F.L.: The development of a nitrogen dioxide sonde. Atmos. Meas. Tech. (2010). doi:10.5194/amt-3-1753-2010

Stauffer, R.M., Thompson, A.M., Martins, D.K., Clark, R.D., Goldberg, D.L., Loughner, C.P., Delgado, R., Dickerson, R.R., Stehr, J.W., Tzortziou, M.A.: Bay breeze influence on surface ozone at Edgewood, MD during July 2011. J. Atmos. Chem. (2012). doi:10.1007/s10874-012-9241-6

Steinbacher, M., Zellweger, C., Schwarzenbach, B., Bugmann, S., Buchmann, B., Ordonez, C., Prevot, A.S.H., Hueglin, C.: Nitrogen oxide measurements at rural sites in Switzerland: Bias of conventional measurement techniques. J. Geophys. Res.-Atmos. (2007). doi:10.1029/2006JD007971

Thompson, A.: The oxidizing capacity of the Earth's atmosphere—probable past and future changes. Science **256**, 1157–1165 (1992)

van den Hooven, E.H., Pierik, F.H., de Kluizenaar, Y., Willemsen, S.P., Hofman, A., van Ratingen, S.W., Zandveld, P.Y.J., Mackenbach, J.P., Steegers, E.A.P., Miedema, H.M.E., Jaddoe, V.W.V.: Air pollution exposure during pregnancy, ultrasound measures of fetal growth, and adverse birth outcomes: A prospective cohort study. Environ. Health Perspect. (2012). doi:10.1289/ehp.1003316

Villena, G., Bejan, I., Kurtenbach, R., Wiesen, P., Kleffmann, J.: Interferences of commercial NO_2 instruments in the urban atmosphere and in smog chamber. Atmos. Meas. Tech. (2012). doi:10.5194/amt-5-149-2012

Volten, H., Brinksma, E.J., Berkhout, A.J.C., Hains, J., Bergwerff, J.B., Van der Hoff, G.R., Apituley, A., Dirksen, R.J., Calabretta-Jongen, S., Swart, D.P.J.: NO_2 lidar profile measurements for satellite interpretation and validation. J. Geophys. Res. (2009). doi:10.1029/2009JD012441

Wang, S., Pongetti, T.J., Sander, S.P., Spinei, E., Mount, G.H., Cede, A., Herman, J.: Direct Sun measurements of NO_2 column abundances from Table Mountain, California: Intercomparison of low- and high-resolution spectrometers. J. Geophys. Res.-Atmos. (2010). doi:10.1029/2009JD013503

Winer, A., Peters, J., Smith, J.P., Pitts, J.N.: Response of commercial chemiluminescent NO-NO_2 anlyzers to other nitrogen-containing compounds. Environ. Sci. Technol. **8**, 1118–1121 (1974)

Yang, S., Yuesi, W., Zhang, C.: Vertical observations and analysis of $PM_{2.5}$, O_3, and NO_x at Beijing and Tianjin from Towers during Summer and Autumn 2006. Adv. Atmos. Sci. **27**, 123–136 (2010)

Zhang, Q., Streets, D.G., He, K., Wang, Y., Richter, A., Burrows, J.P., Uno, I., Jang, C.J., Chen, D., Yao, Z., Lei, Y.: NO(x) emission trends for China, 1995–2004: The view from the ground and the view from space. J. Geophys. Res.-Atmos. (2007). doi:10.1029/2007JD008684